Soil metabolomics and bacterial functional traits revealed the responses of rhizosphere soil bacterial community to long-term continuous cropping of Tibetan barley

Yuan Zhao [Equal first author, 1] , **Youhua Yao** [Equal first author, 2] , **Hongyan Xu** [1, 2] , **Zhanling Xie** [Corresp., 1] , **Jing Guo** [1] , **Zhifan Qi** [1] , **Hongchen Jiang** [3]

[1] Qinghai University, College of Eco-Environmental Engineering, Xining, Qinghai, China

[2] Qinghai University, Academy of Agriculture and Forestry Sciences, Xining, Qinghai, China

[3] China University of Geosciences, State Key Laboratory of Biogeology and Environmental Geology, Wuhan, Hubei, China

Corresponding Author: Zhanling Xie
Email address: xiezhanling2012@126.com

Continuous cropping often leads to an unbalanced soil microbial community, which in turn negatively affects soil functions. However, systematic research of how these effects impact the bacterial composition, microbial functional traits, and soil metabolites is lacking. In the present study, the rhizosphere soil samples of Tibetan barley continuously monocropped for 2 (CCY02), 5 (CCY05), and 10 (CCY10) years were collected. By utilizing 16S high-throughput sequencing, untargeted metabolomes, and quantitative microbial element cycling smart chips, we examined the bacterial community structure, soil metabolites, and bacterial functional gene abundances, respectively. We found that bacterial richness (based on Chao1 and Phylogenetic Diversity [PD] indices) was significantly higher in CCY02 and CCY10 than in CCY05. As per principal component analysis (PCA), samples from the continuous momocropping year tended to share more similar species compositions and soil metabolites, and exhibited distinct patterns over time. The results of the Procrustes analysis indicated that alterations in the soil metabolic profiles and bacterial functional genes after long-term continuous cropping were mainly mediated by soil microbial communities ($P < 0.05$). Moreover, 14 genera mainly contributed to the sample dissimilarities. Of these, five genera were identified as the dominant shared taxa, including *Blastococcus*, *Nocardioides*, *Sphingomonas*, *Bacillus*, and *Solirubrobacter*. The continuous cropping of Tibetan barley significantly increased the abundances of genes related to C-degradation ($F = 9.25$, $P = 0.01$) and P-cycling ($F = 5.35$, $P = 0.03$). N-cycling significantly negatively correlated with bacterial diversity ($r = -0.71$, $P = 0.01$). The co-occurrence network analysis revealed that nine hub genera correlated with most of the functional genes and a hub taxon, Desulfuromonadales, mainly co-occurred with the metabolites via both negative and positive correlations. Collectively, our findings indicated that continuous

cropping significantly altered the bacterial community structure, functioning of rhizosphere soils, and soil metabolites, thereby providing a comprehensive understanding of the effects of the long-term continuous cropping of Tibetan barley.

1 **Soil Metabolomics and Bacterial Functional Traits Revealed the**

2 **Responses of Rhizosphere Soil Bacterial Community to Long-term**

3 **Continuous Cropping of Tibetan Barley**

6 Yuan Zhao[#1], YouhuaYao[#2], Hongyan Xu[1, 2], Zhanling Xie*[1], Jing Guo[1], Zhifan Qi[1], Hongchen

7 Jiang[3]

9 [1]College of Eco-Environmental Engineering, Qinghai University, Xining, Qinghai, China

10 [2]Academy of Agriculture and Forestry Sciences, Qinghai University, Xining, Qinghai, China

11 [3]State Key Laboratory of Biogeology and Environmental Geology, China University of

12 Geosciences, Wuhan, China

14 Corresponding Author:

15 Zhanling Xie [1]

16 Ningda Road 251, Xining, Qinghai, 810016, China

17 Email address: xiezhanling2012@126.com

Abstract

20 Continuous cropping often leads to an unbalanced soil microbial community, which in turn

21 negatively affects soil functions. However, systematic research of how these effects impact the

22 bacterial composition, microbial functional traits, and soil metabolites is lacking. In the present

23 study, the rhizosphere soil samples of Tibetan barley continuously monocropped for 2 (CCY02),

24 5 (CCY05), and 10 (CCY10) years were collected. By utilizing 16S high-throughput sequencing,

25 untargeted metabolomes, and quantitative microbial element cycling smart chips, we examined

26 the bacterial community structure, soil metabolites, and bacterial functional gene abundances,

27 respectively. We found that bacterial richness (based on Chao1 and Phylogenetic Diversity [PD]

28 indices) was significantly higher in CCY02 and CCY10 than in CCY05. As per principal

29 component analysis (PCA), samples from the continuous momocropping year tended to share

30 more similar species compositions and soil metabolites, and exhibited distinct patterns over time.

31 The results of the Procrustes analysis indicated that alterations in the soil metabolic profiles and

32 bacterial functional genes after long-term continuous cropping were mainly mediated by soil

33 microbial communities ($P < 0.05$). Moreover, 14 genera mainly contributed to the sample

34 dissimilarities. Of these, five genera were identified as the dominant shared taxa, including

35 *Blastococcus*, *Nocardioides*, *Sphingomonas*, *Bacillus*, and *Solirubrobacter*. The continuous

36 cropping of Tibetan barley significantly increased the abundances of genes related to C-

37 degradation ($F = 9.25$, $P = 0.01$) and P-cycling ($F = 5.35$, $P = 0.03$). N-cycling significantly
38 negatively correlated with bacterial diversity ($r = -0.71$, $P = 0.01$). The co-occurrence network
39 analysis revealed that nine hub genera correlated with most of the functional genes and a hub
40 taxon, Desulfuromonadales, mainly co-occurred with the metabolites via both negative and
41 positive correlations. Collectively, our findings indicated that continuous cropping significantly
42 altered the bacterial community structure, functioning of rhizosphere soils, and soil metabolites,
43 thereby providing a comprehensive understanding of the effects of the long-term continuous
44 cropping of Tibetan barley.
45 **Keywords:** Tibetan barley; continuous cropping; rhizosphere bacterial community;
46 metabolomics; elemental cycling genes.
47

48 **Introduction**
49 Soil health sustains the capacity of agricultural soils for ecosystem functioning and thrives as a
50 living ecosystem for microbes, plants, and insects (Lal 2016; Rinot et al. 2019). However,
51 continuous cropping, especially of a monoculture consisting of one plant type in the same
52 agricultural field with standard and persistent agronomic practices, usually leads to crop yield
53 reductions, soil aggregation, soil physicochemical property alterations, and soil microbial
54 community changes, ultimately exerting negative effects on soil health (Murphy & Lemerle
55 2006; Pervaiz et al. 2020). Soil microbiota play crucial roles in the maintenance of soil functions
56 and prominently affect agricultural soil productivity, plant growth, and crop quality (Bello-
57 Akinosho et al. 2016; Huang et al. 2013; Pii et al. 2016). Previous studies demonstrated that
58 continuous monoculture greatly affected the structure of the rhizosphere soil microbial
59 community. For example, successive monoculture practices were found to decrease bacterial
60 community diversity (Sun et al. 2018), increase harmful populations, and inhibit beneficial ones
61 (Gao et al. 2019). In our previous study, we found that the continuous cropping of Tibetan barley
62 resulted in a significant decline in crop yields and bacterial community diversity, as well as
63 increased the relative abundances of bacteria associated with chemo-heterotrophy, aromatic
64 compound degradation, and nitrate reduction, per a FaProTax prediction (Yao et al. 2020).
65 However, research on how continuous cropping practices affect soil microbial functional traits is
66 lacking.
67 Nutrient cycling, including carbon (C), nitrogen (N), and phosphorus (P), is a common problem
68 that has been investigated on a global scale (Zhang et al. 2019). The tight interactions in the
69 rhizosphere zone between plants and soil microbiota affect the stability of nutrient cycling in the
70 soil (Zhang et al. 2019). For example, Kuzyakov et al. (2010) reported that soil microbial activity
71 was enhanced by a substantial source of soil C from root secretion and deposition. Yu et al.
72 (2019) found that the activities of key functional genes within the microbial community involved
73 in N-cycling increased along with a reduction in N application during maize/soybean strip

74   intercropping. Alami et al. (2020) found that the abundances of soil N functional genes
75   significantly differed between cultivated and fallow fields across two seasons based on a
76   PICRUSt prediction. Pang et al. (2021) indicated that the continuous cropping of sugarcane
77   significantly decreased the bacterial abundances associated with rhizosphere soil N- and sulfur
78   (S)-cycling, thereby decreasing the abundances of N translocation genes and dissimilatory
79   reduction genes, as determined by the soil metagenome. Unfortunately, less is known about soil
80   functional gene cycling and their interactions with microbial communities underlying the
81   continuous cropping of Tibetan barley.
82   Most studies on continuous cropping have generally focused on changes in the microbial
83   community and their interactions with soil properties, while soil metabolite composition is rarely
84   discussed. The rhizosphere, which is a hub of microbial activities, increases the nutrient supply
85   for microorganisms, as the roots release several organic compounds that influence plant growth
86   and health (Pinton et al. 2007). Thus, soil metabolomics can potentially enhance our
87   understanding of this chemical exchange. Fortunately, the development of untargeted
88   metabolomics has allowed us to detect and identify increasingly more compounds that are
89   secreted by plants and the organisms that interact with them in the rhizosphere (Swenson et al.
90   2015; Withers et al. 2020). For example, Wang et al. (2020) studied the continuous cropping of
91   ramie by combining rhizosphere microbe identification and non-targeted gas chromatograph-
92   mass spectrometer (GS/MS) metabolome analysis, and found that bacteria, such as Rhizobia,
93   synthesized IAA and likely reduced the biotic stress of ramie. Nevertheless, the contribution of
94   the changes in soil metabolites, their co-occurrence network, and microbial composition on the
95   long-term monoculture of crops are far less understood, especially in Tibetan barley.
96   Thus, in the present study, we collected the rhizosphere soils of Tibetan barley after two short-
97   term and one long-term periods of cropping. By applying high-throughput sequencing and liquid
98   chromatography mass spectrometry (LC-MS) untargeted metabolomics, we investigated the
99   change trends in soil bacterial community structures and differences in soil metabolites. By
100   constructing a co-occurrence network, we determined the changes in the interactions of bacterial
101   communities. Quantitative microbial element cycling (QMEC) was applied to detect the
102   abundances of C-, N-, P-, and S-cycling-related genes in the rhizosphere soils of different
103   continuous cropping years (Zheng et al. 2018). Our findings will enhance our understanding of
104   the effects of the long-term continuous cropping of Tibetan barley on the direct interactions
105   between specific functional taxa and important functional gene metabolism, and provide a
106   comprehensive understanding of the effects of the long-term continuous cropping of Tibetan
107   barley.
108

109   **Materials & Methods**
110   **Site description and rhizosphere soil sampling**

111   The study was carried out at an alpine Tibetan barley experiment site located in the Qinghai–
112   Tibetan Plateau (37°21′N, 101°43′E; altitude, 3700 m), Beishan Township, Menyuan County,
113   Qinghai Province, China. This region has a plateau continental climate with a mean annual
114   temperature of 1.3°C and mean annual precipitation of 530–560 mm. According to the Food and
115   Agriculture Organization (FAO) classification, the soil type is classified as Kastanozems (Schad
116   & Spaargaren 2006). Kunlun 14 barley (Hordeum vulgare L.) was used as the experiment
117   material. The study site consisted of independent plots over many years of the successive
118   monoculture of Tibetan barley. Tibetan barley seeds were cultivated in April each year after the
119   annual application of blended fertilizer and harvested in August following previously described
120   methods (Yao et al. 2020). Briefly, in July 2020, we selected three 5 m × 5 m quadrats including
121   2, 5, and 10 years of successive monocropping of Tibetan barley, which we named CCY02,
122   CCY05, and CCY10, respectively. Each quadrat was originally divided into five rectangular 5 m
123   × 1 m sub-quadrats. In each sub-quadrat, we collected a total of 15 rhizosphere soil samples
124   (closely adhered to the roots) in a "Z" pattern and all rhizosphere soil samples within a quadrat
125   were mixed together as a single biological sample. The same steps were repeated four times to
126   make four biological rhizosphere soil duplicates per continuous monocropping year. Finally, we
127   obtained a total 12 rhizosphere soil samples for the subsequent experiments. Soil samples were
128   then immediately transferred on ice to the laboratory and stored at -20°C for subsequent analysis.
129

130   **High-throughput sequencing of bacterial 16S rRNA gene**
131   The genomic DNA was extracted from each rhizosphere soil sample using an E.Z.N.A. ® Soil
132   DNA kit (Omega Bio-Tek, Norcross, GA, USA) following the manufacturer's instructions. The
133   bacterial V3-4 region was then amplified with the primer set 338F (5'-ACT CCT ACG GGA
134   GGC AGC AG-3') and 806R (5'-GGA CTA CHV GGG TWT CTA AT-3') (Zeng & An 2021).
135   PCR amplification and purification were performed following previously described methods
136   (Yang et al. 2019). Briefly, each sample consisted of a 30 μL mixture in triplicate, comprised of
137   10 μL TaKaTa EX Tag PCR premix (TaKaRa Bio Inc., Kusatsu, Japan), 0.5 μL of each primer
138   (10 μM), 1 μL DNA template (20 ng), and 18 μL PCR-grade water, which was amplified
139   according to the stetted procedure (95°C for 5 min, followed by 25 cycles at 95°C for 30 s, 55°C
140   for 30 s, 72°C for 30 s, and a final extension at 72°C for 10 min). The replicate PCR reactions for
141   each triplicate were pooled and purified using a QIAquick Gel Extraction Kit (Qiagen,
142   Chatsworth, CA, USA). A single composite sample for sequencing was prepared by combining
143   approximately equimolar amounts of PCR products from each sample. The prepared PCR
144   products were then paired-end sequenced (2× 250 bp) on an Illumina MiSeq platform (Majorbio
145   Biotech CO., Ltd., Shanghai, China) following the manufacturer's instructions.
146

147   **Soil non-targeted metabolomic detection and analysis**

Manuscript to be reviewed

148 Twelve rhizosphere soil samples were sent to Majorbio (Shanghai, China) on dry ice for

149 metabolite extraction, detection, and analysis. In detail, 1,000-mg soil aliquot of each sample was

150 homogenized with 1,000 μL methanol/water (4:1, v/v) solution, including 0.02 mg/mL internal

151 standard (L-2-chlorophenylamine acid) for 6 min at −10°C and 50 kHz using a Geno-grinder

152 2,000 (SPEX, Metuchen, NJ, USA) and spun down for 30 min at 5°C and 40 kHz. After placing

153 for 30 min at −20°C, each material was centrifuged at 13,000 g (relative centrifugal force) for 15

154 min at 4°C, then the supernatant was transferred and concentrated by a Termovap Sample

155 Concentrator (DC-24, Anpel Laboratory Technologies, Shanghai, China). The dry residue was

156 derivatized by adding 50 μL acetonitrile/water (1:1), homogenized for 30 s at 5°C and 40 kHz,

157 and centrifuged at 13,000 g (relative centrifugal force) for 10 min at 4°C. Finally, the supernatant

158 was subjected to LC-tandem MS (MS/MS) analysis; 20 μL supernatant of each sample was

159 mixed for the quality control sample.

160 The UHPLC-Triple TOF system (AB Sciex, Foster City, CA, USA) equipped with an

161 ACQUITY UPLC HSS T3 (100 mm × 2.1 mm i.d., 1.8 μm; Waters, Milford, CT, USA) was

162 applied to chromatographic separating the metabolites with two mobile phases, phase A (95%

163 water and 5% acetonitrile (with 0.1% formic acid)) and phase B (5% water (with 0.1% formic

164 acid), 47.5% acetonitrile, and 47.5% isopropanol). The whole system was integrated to a

165 quadrupole time-of-flight mass spectrometer (Triple TOFTM 5600þ; AB Sciex, Foster City, CA,

166 USA) equipped with an electrospray ionization source and operated in positive and negative

167 modes.

168 The online analysis platform (Majorbio, Shanghai, China) was applied to the raw data following

169 the manufacturer's instructions. Briefly, the ProgenesisQI (Waters Corp., Milford, CT, USA)

170 was used for baseline filtering, peak recognition, integration, retention time correction, and peak

171 alignment, which produced the retention time, mass charge ratio, peak intensity, and data matrix.

172 Then, the characteristic peak was detected and the information from the MS and MS/MS

173 analyses was mapped with a metabolic specific database; the mass error was set to < 10 PPM.

174 Finally, the metabolites were identified according to the matching scores of the secondary MS.

175 The data were normalized with Pareto scaling and log-transformed before further analysis.

176

177 **QMEC**

178 Twelve qualified soil DNA samples were sent to Guangdong Magigene Biotechnology Co., Ltd.

179 (Guangzhou, China) for QMEC analysis, wherein a high-throughput quantitative PCR (qPCR)-

180 based chip was applied to assess the microbial functional potential, including 71 functional genes

181 related to C-, N-, P-, and S-cycling (Zheng et al. 2018). QMEC manipulation was conducted

182 following previously described methods (Chen et al. 2020a). Briefly, DNA templates and qPCR

183 reagents were added to the sample source-plate; each primer and qPCR reagent was added to a

184 separate source-plate. In each run, using a non-template reaction as the negative control, 100-nL

185   reactions were mixed in parallel three times using an automated high-throughput sample

186   preparation device, and then added to the nanopore of the qPCR chip on a Wafergen Smart-Chip

187   Real-time PCR platform (Wafergen, Fremont, CA, USA). Specifically, a threshold cycle (CT) of

188   31 was used as the detection limit and multiple melting peaks; amplification efficiencies outside

189   the range of 0.9–1.1 were discarded.

190

191   **Data and statistical analyses**

192   The 16S rRNA gene raw reads were processed by the QIIME2 v2020.08 pipeline (Bolyen et al.

193   2019). Briefly, paired-end reads were joined by FLASH v1.2.11 (Magoč & Salzberg 2011), then

194   sequences were demultiplexed by the q2-demux plugin. Afterwards, plugin q2-dada2 was used to

195   conduct quality control, chimeric sequence removal, and sequence clustering. Taxonomic

196   analyses were conducted using the plugins q2-feature-classifier and SILVA v132 database

197   (Quast et al. 2012). The α diversity of the bacterial communities was represented by the Chao1,

198   Shannon, ACE, and Faith's phylogenetic diversity (PD) indices, which were calculated from the

199   amplicon sequence variants (ASVs) table rarefied to 20,349 sequences in QIIME2 for each

200   sample.

201   Beta diversity metrics differ widely in the types of differences they detect, therefore, four

202   distance-based principal coordinate analysis (PCoA), including the Bray–Curtis, Jaccard,

203   Weighted Unifrac, and Unweighted Unifrac were applied to visualize the differentiation among

204   samples. Non-parametric multivariate statistical tests, Kruskal-Wallis or Adonis, were

205   implemented to test for significant differences between the variances of bacterial communities

206   with a $P < 0.05$ significance threshold. The similarity of percentages analysis (SIMPER) was

207   applied to identify the most affected genus between different continuous cropping years using

208   the R package, Vegan (Oksanen et al. 2013). Procrustes included in the Vegan R package was

209   used to compare the congruence of the microbiome and metabolism or functional profiles based

210   on the P-values and goodness of fit (m^2). The co-occurrence network construction and parameter

211   statistics were performed using Cytoscape v3.9.0 software (Shannon et al. 2003). The network

212   was visualized using the interactive platform, Gephi (Cherven 2013). In each network, the node

213   size (i.e., degrees) was proportional to its number of connections; the thickness of each

214   connection between two nodes (i.e., edges) was proportional to the Spearman's correlation

215   coefficient ($|r| = 0.6$–1).

216

217   **Sequence accessions**

218   The bacterial 16S rRNA gene sequencing data are publicly available in the NCBI Short Read

219   Archive (SRA) under Bioproject accession No.: PRJNA759342.

220

221   **Results**

Overall measures of diversity

We obtained 503,330 raw sequences and an average of 41,944 sequences per sample. After quality control and sample normalization, a total of 244,188 sequences were filtered and clustered into 6,745 unique ASVs (Edgar 2018). The coverage of samples was > 93% and the rarefaction curve of each sample approached a saturation plateau (Fig. S1), indicating that the current sequencing depth reflected the microbial composition. The Chao1, ACE, and PD indices were all significantly higher in CCY02 and CCY10 compared with CCY05 (all $P<0.05$) (Table 1). The Shannon index was significantly higher in CCY10 when compared to CCY05, but no significant differences existed between CCY10 and CCY02, or CCY02 and CCY05, indicating that the bacterial diversity measured by the species richness with evenness had been reduced, but was not significant, during short continuous cropping years; after longer monocropping years, the whole bacterial diversity seemed to recover.

According to four different distance-based PCoA, we found that samples from the same cropping year clustered tightly, while samples from different years clearly separated based on both Jaccard (Fig. S2A) and Unweighted UniFrac PCoA (Fig. S2B), indicating that there clear differences existed in the absence or presence of ASVs among groups. Meanwhile, we found by Bray-Curtis PCoA (Fig. S2C) that, when considering the presence, absence, and abundance of ASVs, CCY05 obviously separated from CCY02 and CCY10. Additionally, there were no obvious differences detected among communities per the Weighted-Unifrac distances (Fig. S2D), which considered the presence, absence, abundance, and up-weighting differences in distant evolutionarily-related ASVs. Furthermore, the soil microbial compositions under different treatments were analyzed by Adonis statistical tests, which revealed significant dissimilarities among different cropping years (Table S1).

Microbial community composition

Overall, Actinobacteria (average ± standard deviation (SD), 28.84 ± 1.50%) and Proteobacteria (26.88 ± 1.50%) were the dominant phyla across all rhizosphere soil samples. The genera with relative abundances > 1% included *Blastococcus* (2.57 ± 0.30%), *Nocardioides* (2.55 ± 0.39%), *Sphingomonas* (2.44 ± 0.28%), *Bacillus* (1.09 ± 0.30%), and *Solirubrobacter* (1.02 ± 0.04%), but these genera did not significantly differ among continuous cropping years. After comparing the relative abundances of each known taxa among the 3 successive monoculture years, we found that 6 phyla, 5 classes, 11 orders, 23 families, and 47 genera exhibited a straight increasing trend over time, while 5 phyla, 8 classes, 14 orders, 19 families, and 32 genera exhibited the opposite trend. A total of 20 taxa exhibited significant continuously strengthened or weakened tolerance to the long-term continuous cropping of Tibetan barley based on the ANOVA results (Fig. 1), but most of these taxa were low in abundance with a mean relative abundance < 1%. For example, Fibrobacteres is an important phylum of cellulose-degrading bacteria (Ransom-Jones et

259   al. 2012); the genus *Devosia* possesses bioremediation potential (Talwar et al. 2020); and the
260   denitrifying bacteria *Noviherbaspirillum* (Wu et al. 2021) were significantly upregulated over
261   time. The following significantly decreased over time: Firmicutes, which are plant growth-
262   promoting bacilli (Kumar et al. 2012); Bacillales, which have effective biological control and
263   biodegradation potential (Barathi et al. 2020); Nitrosomonadales, which are related to sulfate and
264   iron reduction; and Desulfuromonadales, which are an order capable of iron and sulfate reduction
265   (Wunder et al. 2021).
266   A SIMPER analysis was used to detect the main genera that drove the compositional shifts of
267   bacterial communities over time. The results showed that 22, 24, and 25 genera were responsible
268   for > 50% cumulative dissimilarity of the microbial community shifts between CCY02 and
269   CCY05, CCY02 and CCY10, and CCY05 and CCY10, respectively (Fig. 2). Fourteen of these
270   overlapping genera were mainly responsible for the differences between each pair of cropping
271   years (Table S2), and the genera *Nocardioides* had the largest dissimilarity contribution.
272
273   **Core taxa among different cropping years**
274   The consistency of crop type, planting strategies, and research site may lead to a cohort of
275   rhizosphere soil-shared microbial communities from Tibetan barley, while continuous cropping
276   over time could lead to year-unique taxa in the rhizosphere soil. In this study, the taxa that were
277   simultaneously present in all samples were defined as core or shared taxa, and when their mean
278   relative abundances (at the genus level) were > or < 1%, they were defined as dominant or rare
279   core taxa and subsequently classified at the phylum, class, order, family, and genus levels (Gobet
280   et al. 2010). At the genus level, the core shared microbiome consisted of nearly 50.87% of all
281   taxa (taxonomic richness) and this percentage reached 60% at the phylum level, however, a
282   proportion of unshared taxa seemed to be sample-specific (Fig. 3A). Surprisingly, the total
283   relative abundances of the core taxa at the genus level occupied > 98% of all sequences on
284   average (Fig. 3A), while unshared taxa, or sample-unique taxa, only occupied 1.66 ± 0.31% of
285   all sequences. A total of 164 core taxa were successfully annotated at the genus level and the
286   relative abundances ranged from 0.02 ± 0.01% to 2.57 ± 0.61% (Table S3). The dominant shared
287   genera among samples were *Blastococcus*, *Nocardioides*, *Sphingomonas*, *Bacillus*, and
288   *Solirubrobacter* (Fig. 3B).
289
290   **Bacterial functional genes**
291   QMEC was implemented to determine the abundances of a wide spectrum of functional genes
292   related to C-, N-, P-, and S-cycling (71 genes in total) in a high-throughput manner. A total of 60
293   genes were successfully detected by QMEC across 12 samples, including 17 genes related to C-
294   degradation, 13 related to C-fixation, 19 related to N-cycling, 6 related to P-cycling, and 5
295   related to S-cycling (Table S4). Samples from CCY02 and CCY10 displayed a clear clustered

296   pattern based on the principal components analysis (PCA), while samples from CCY05 were
297   scattered (Fig. S3). The abundances of each gene in 12 samples are presented in Fig. S4. Briefly,
298   we found that the genes involved in hemicellulose degradation (*abfA* and *xylA*) were most
299   prevalent in C-degradation. The gene involved in the Wood–Ljungdahl pathway (*acsA*) and the
300   gene involved in ammonization (*UreC*) were most abundant in C-fixation and N-cycling,
301   respectively. In P-cycling, the genes involved in organic P mineralization (*phoD* and *phnK*) were
302   the dominant genes across samples, while the gene related to S reduction (*apsA*) and the genes
303   (*YedZ* and *SoxY*) related to S oxidation were the main genes in S-cycling.
304   We employed Z-values to compare differences in cycling genes among different cropping years
305   (Table S5). The long-term continuous cropping of Tibetan barley significantly increased the
306   abundances of genes related to C-degradation ($F = 9.25$, $P = 0.01$) and P-cycling ($F = 5.35$, $P =$
307   0.03) (Fig. S5A and S5B). The abundances of N-cycling genes increased from CCY02 to CCY05
308   and decreased by CCY10, but no significant differences were detected between groups (Fig.
309   S5C). We also investigated the relationship between the abundances of functional genes and
310   bacterial diversity (Shannon) (Table S6). Results revealed that only N-cycling significantly
311   correlated with bacterial diversity ($r = −0.71$, $P = 0.01$).
312
313   **Relationships between taxa and functional genes**
314   The Procrustes analysis showed that there were significant correlations between bacterial
315   composition and functional gene profiles after long-term continuous cropping ($P = 0.012$) (Fig.
316   4A), but not after short-term continuous cropping ($P = 0.111$) (Fig. 4B). A co-occurrence
317   network was constructed to visualize the relationships between the functional cycling genes and
318   bacterial genera (Fig. 5). Only the interactions between the genera and functional genes were
319   kept, of which 173 nodes and 481 edges (196 positive and 285 negative associations) were
320   obtained. The network had good modularity (0.41) and contained 6 modules; each included
321   tightly connected nodes. Module I, which was the largest, contained 65 nodes, including 43
322   functional genes and 22 genera; most of the C-, N-, P-, and S-cycling genes were tightly
323   connected with a small group of genera. Nine key genera with a degree value > 10 were
324   identified, including *Saccharothrix*, *Planomicrobium*, *Edaphobaculum*, *Nitrosospira*,
325   *Angustibacter*, *Sanguibacter*, *Brevibacillus*, *Caulobacter*, and *Pantoea*. Interestingly,
326   *Saccharothrix*, *Edaphobaculum*, *Sanguibacter*, and *Pantoea* were positively connected with the
327   functional genes, while *Planomicrobium*, *Nitrosospira*, *Angustibacter*, *Brevibacillus*, and
328   *Caulobacter* were mainly negatively connected (Table S7).
329   We also examined the correlations between the cycling genes and 14 top contributors with the
330   dissimilarities among different cropping years. Results revealed that *Ohtaekwangia* ($r = 0.64$, P
331   = 0.02), *Pedobacter* ($r = 0.63$, $P = 0.03$), and *Gaiella* ($r = 0.63$, $P = 0.03$) significantly positively
332   correlated with *gmGDH*, which is related to C degradation (Fig. 6). With regard to C fixation,

333   *Devosia* significantly positively correlated with *cdaR* ($r = 0.66$, $P = 0.02$), while *Gaiella*

334   significantly positively correlated with *frdA* ($r = 0.58$, $P = 0.04$) and *rbcL* ($r = 0.68$, $P = 0.01$).

335   For N-cycling, *Devosia* and *Sphingomonas* significantly negatively correlated with *amoA2* and

336   *nxrA* ($P < 0.05$), while *Saccharibacillus* significantly positively correlated with these genes ($P <$

337   0.05). For P-cycling, *Blastococcus* significantly negatively correlated with *dsrB* ($r = -0.58$, $P =$

338   0.04), while *Marmoricola* significantly positively correlated with *phnK* ($r = 0.60$, $P = 0.04$). No

339   significant correlations were detected between the five major categories of functional genes and

340   14 top genera (Fig. S6).

341

342   **Soil metabolic profiles**

343   By LC-MS/MS-based non-targeted metabolomics, a total of 14,380 metabolites in the soils were

344   obtained, in which, 822 metabolites were successfully annotated in the HMDB and KEGG

345   databases. Based on the metabolic profiles, we implemented a PCA to uncover the different

346   compositions of metabolites in the soil samples from different continuous cropping years.

347   Results revealed that the first two principal components (PC1 and PC2) explained 62.93% of the

348   total variance and samples from different groups obviously differed from each other (Fig. S7).

349   The varying metabolic compositions among different groups were further confirmed by the

350   heatmap analysis of the top 100 metabolites (Fig. S8).

351   VIP values in the PLS-DA model were calculated to examine the changes in the soil metabolites

352   in greater detail. A total of 440 metabolites with VIP > 1.0 and $P < 0.05$ (ANOVA) were

353   considered significantly affected by the continuous cropping of Tibetan barley. Further linear

354   regression analyses between the acquired metabolites and enhanced continuous cropping years

355   were conducted. A total of 126 metabolites significantly responded to continuous cropping with

356   an increase in 83 metabolites and decrease in 43 metabolites (Table S8). The changes in

357   metabolites mainly occurred in lipids and lipid-like molecules, organic acids and derivatives, and

358   organoheterocyclic compounds. Lipids and lipid-like molecules had the largest number of

359   metabolites affected by continuous cropping. Moreover, nucleosides, nucleotides, and analogues

360   were mainly upregulated over time, while alkaloids and derivatives were mainly downregulated.

361

362   **Relationships between taxa and metabolites**

363   First, we applied Procrustes tests to depict the correlations between soil metabolic profiles and

364   the bacterial community structure. Significant correlations were detected between specific

365   metabolites and the bacterial community structure in rhizosphere soils during the long- ($P =$

366   0.001) and short-term continuous cropping of Tibetan barley ($P = 0.027$) (Fig. 7). To elucidate

367   which microbial taxa were responsible for the changes in soil microbial metabolism, an

368   interactive network linking the microbes with significant differences between groups (a total of

369   100 microbial taxa) and differential metabolites (a of total 126 metabolites) was constructed.

370   Only the interactions between metabolites and microbial taxa were kept. The orders
371   Desulfuromonadales (degree 57) and Nitrosomonadales (degree 19), families Archangiaceae
372   (degree 34), Nocardiaceae (degree 23), and Sanguibacteraceae (degree 11), and genera
373   *Terrimicrobium* (degree 35), *Caldinitratiruptor* (degree 34), *Dehalogenimonas* (degree 21),
374   *Rubellimicrobium* (degree 15), *Aquimonas* (degree 13), and *Sanguibacter* (degree 11) co-
375   occurred most frequently with several differential metabolites, including 4-hydroxyvalsartan,
376   methyl-4-pentanoate, pentigetide, and glaucarubolone-15-O-beta-D-glucopyranoside (Fig. 8). Of
377   these metabolites, the frequently co-occurring ones were downregulated over time, except 4-
378   hydroxyvalsartan.
379

Discussion

Effects of continuous cropping on microbial community structure and diversity

382   Long-term continuous cropping may significantly alter bacterial community structure and
383   diversity. For instance, Yan et al. (2021) reported that soil bacterial diversity significantly
384   decreased (PD and Shannon) after the continuous cropping of *Nicotiana tabacum*. Chen et al.
385   (2020b) found that the long-term consecutive monocropping of peanuts led to a general, albeit
386   insignificant, loss in bacterial diversity. Liu et al. (2020) found that the bacterial diversity (PD
387   and number of operational taxonomic units (OTUs)) was significantly higher after the long-term
388   (13 year) continuous monoculture of soybeans, while no significant differences were detected
389   after the short-term monoculture periods (3 and 5 years). Zhao et al. (2020) showed that bacterial
390   richness (ACE) significantly decreased after 5–10 years of continuous cropping and recovered
391   after 30 years, while bacterial diversity (Shannon) significantly increased after continuous
392   cropping (5, 10, and 30 years). In the present study, bacterial diversity (Shannon) did not differ
393   during short continuous cropping years, but bacterial richness (Chao1 and ACE) and PD
394   significantly declined after short-term continuous cropping of Tibetan barley, which is consistent
395   with the findings of Yao et al. (2020), but surprisingly recovered after long-term continuous
396   cropping (Table 1). This phenomenon may be due to the fact that all environmental filters require
397   specific adaptation strategies for survival; stronger selection acting on bacteria often leads to a
398   new cohort of microbiota that adapt to the environment (Fierer et al. 2007; Meola et al. 2014).
399   Even if the microbial composition is sensitive to environmental disturbances, the community
400   may be resilient and stabilize over time (Allison & Martiny 2008). However, we believe that the
401   application of more powerful methods (e.g. metagenome and metagenome binning) to deeply
402   investigate the reasons for this phenomenon in future studies.
403   After 10 years of continuous cropping of Tibetan barley, Actinobacteria and Proteobacteria were
404   the two main dominant phyla that were enriched in many rhizosphere soils after continuous
405   cropping, such as in sugarcane and cotton (Pang et al. 2021; Xi et al. 2019). The widely
406   distributed bacterial phyla, Actinobacteria, possess high proportions of CAZymes and exhibited

407   a key important eco-physiological role in plant residue decomposition in a previous study (Bao et
408   al. 2021). Another abundant phylum, Proteobacteria, plays a central role in the cycling of several
409   key elements, including N- (Conthe et al. 2018), C- (Chan et al. 2013), and S-cycling (Zhou et al.
410   2020). In this study, a total of 20 low abundant taxa (< 1%) significantly increased after
411   continuous cropping, during which planting-promoting bacteria or bacteria with bioremediation
412   abilities significantly decreased.
413   In the current study, we analyzed the top genera that contributed to the dissimilarities among
414   microbial communities from different continuous cropping years. Of these, five were identified
415   as the dominant shared genera across all soil samples, including *Blastococcus*, *Nocardioides*,
416   *Sphingomonas*, *Bacillus*, and *Solirubrobacter* (Table S2). These genera have been frequently
417   detected in the rhizosphere soils after the continuous cropping of different crops, including maize
418   (Zhao et al. 2021), cucumber (Li et al. 2021), cotton (Han et al. 2017), and peanuts (Chen et al.
419   2018). *Solirubrobacter* and *Blastococcus* exhibit heavy metal tolerance and advantages in stress
420   resistance, indicating the promising potential for alleviating polluted soil ecosystems (Hou et al.
421   2021; Wang et al. 2021). A recent study suggested that *Sphingomonas* possesses multifaceted
422   functions ranging from the remediation of environmental contamination to producing highly
423   beneficial phytohormones that promote plant growth (Asaf et al. 2020). *Bacillus* has multiple
424   medical, environmental, and industrial applications (Khurana et al. 2020). Hence, it is proposed
425   that they may play important roles in the successive monoculture of Tibetan barley.
426
427   **Functional genes and their interactions with microbes**
428   For the first time, QMEC was applied to determine the relative abundances of key element
429   cycling genes after long-term continuous cropping. We found that overall bacterial composition
430   significantly correlated with functional gene profiles (Fig. 4A), indicating that after long-term
431   continuous cropping, and alterations in community functions were mainly affected by alterations
432   in bacterial composition. However, after short-term continuous cropping (CCY02 and CCY05),
433   the functional gene profiles and bacterial compositions had poor consistency (Fig. 4B). Thus, we
434   proposed that the functional gene composition was not mainly mediated by changes in microbial
435   composition after short-term continuous cropping. This may be a result of functional redundancy
436   (Rosenfeld 2002), which contributed to bacterial community tolerance and overall community
437   functioning after the short-term continuous monoculture of Tibetan barley. However, significant
438   fluctuations in the taxonomic composition after the long-term continuous monoculture may
439   potentially reduce the stability of the community, which would thereby become more vulnerable
440   to continuous disturbances (Sheng et al. 2015), ultimately affecting bacterial functional
441   compositions.
442   Genes related to C-degradation and P-cycling increased over time (Table S5). Hemicellulose
443   degradation (*abfA* and *xylA*) was most prevalent in C degradation, indicating the potential loss of

444   soil C storage (Chen et al. 2020a). Organic P mineralization (*phoD* and *phnK*) increased after
445   continuous cropping, playing an important role in soil P bioavailability. Meyer et al. (2018)
446   indicated that microbes compensated for single nutrient deficiencies by accelerating P- or N-
447   cycling and may have increased SOC turnover in co-limited subsoils with acquirable P reserves.
448   Collectively, these results indicated that, along with the continuous cropping of Tibetan barley,
449   the activity of hemicellulose degradation increased and accelerated C degradation, while
450   microbes may have acquired greater C or N supplies by promoting organic P mineralization.
451   Furthermore, a set of genera were identified that showed tight correlations with most of the
452   functional genes, indicating their functional potential in the cycling of key elements underlying
453   the continuous monocropping of Tibetan barley (Fig. 5). In a previous study, *Nitrosospira* was
454   the primary ammonia-oxidizing bacteria and was mainly responsible for nitrous oxide production
455   (Lourenço et al. 2018). *Pantoea* fixes N or induces N uptake, thereby promoting N availability in
456   plants (Loiret et al. 2004; Singh et al. 2020). Additionally, *Brevibacillus* was reported to have
457   desulfurization activity (Nassar et al. 2013).
458   A relevant study pointed out that the continuous cropping of Tibetan barley significantly
459   increased the bacteria associated with chemo-heterotrophy, aromatic compound degradation, and
460   nitrate reduction (Yao et al. 2020). This study showed that the dominant shared genera,
461   *Sphingomonas*, exerted significant negative effects on nitrification gene abundances (*amoA* and
462   *nxrA*), leading to the imbalance of nitrification and denitrification. Additionally, a previous study
463   showed that *Sphingomonas* in vegetable systems utilized contaminants originating from pesticide
464   residues as a growth and energy source (Busse et al. 2003).
465
466   **Soil metabolites and their interactions with microbes**
467   Chemical dialog undergoing rhizosphere active zones promotes the interactions between plant
468   roots and microbial communities (van Dam & Bouwmeester 2016). Shen et al. (2020) observed
469   distinct differences in the metabolite composition over different continuous cropping seasons in
470   tobacco. Our study explored the alterations in soil metabolic profiles, which were significantly
471   mediated by soil microbial communities, indicating that certain metabolic pathways were altered
472   for soil microbial communities to adapt to environmental stress (Fig. 7). Obvious differences in
473   the patterns of metabolite compositions over time were observed (Figs. S7 and S8), in which the
474   primary metabolites related to lipid and nucleoside metabolism were significantly upregulated,
475   while secondary metabolites, such as alkaloids and derivatives, were significantly
476   downregulated. A previous study pointed out that secondary metabolites greatly affect the
477   microbial community, where some metabolites were antibiotic and pharmaceutically relevant,
478   while others were involved in disease interactions (Fox & Howlett 2008).
479   We found that the hub taxa Desulfuromonadales, which was reported to utilize different electron
480   exchange pathways (Rotaru et al. 2012), mainly co-occurred with metabolites in either negative

481 or positive correlations (Fig. 8), indicating potential important interactions between them.
482 Meanwhile, a previous study suggested that positive co-occurrences indicated that the
483 metabolites may have be mainly originated from microbes, while negative co-occurrences may
484 represent the specific microbial consumption or degradation (Devi et al. 2017). These findings
485 indicated that soil metabolomics can be used to assess the adaptations of soil microbial
486 communities to continuous cropping strategies at the molecular level.
487

Conclusions

489 Collectively, we analyzed the changing trends of bacterial composition and diversity after the
490 continuous cropping of Tibetan barley using 16S high-throughput sequencing. After short-term
491 continuous cropping, bacterial richness and PD significantly decreased, but recovered after long-
492 term continuous cropping. We identified five dominant shared genera that were the main
493 contributors to the dissimilarities among bacterial communities from different continuous
494 cropping years, as uncovered by the core taxa and SIMPER analyses. Then, QMEC and
495 untargeted metabolism were employed to determine the main functional genes and soil
496 metabolites, as well as their changing trends after different continuous cropping years. We
497 further predicted the potential correlations between microbiota and metabolism, including
498 functional genes and soil metabolites. Through this study, we gained further insights into the
499 ecological roles of rhizosphere soil microorganisms underlying the continuous cropping of
500 Tibetan barley.
501

Acknowledgements

503   We thank LetPub (www.letpub.com) for its linguistic assistance during the preparation of
504 this manuscript.

505

References

507 Alami MM, Xue J, Ma Y, Zhu D, Gong Z, Shu S, and Wang X. 2020. Structure, diversity, and
508   composition of bacterial communities in rhizospheric soil of coptis chinensis franch
509   under continuously cropped fields. *Diversity* 12:57.
510 Allison SD, and Martiny JB. 2008. Resistance, resilience, and redundancy in microbial
511   communities. *Proceedings of the National Academy of Sciences* 105:11512-11519.
512 Asaf S, Numan M, Khan AL, and Al-Harrasi A. 2020. Sphingomonas: from diversity and
513   genomics to functional role in environmental remediation and plant growth. *Critical*
514   *reviews in biotechnology* 40:138-152.
515 Bao Y, Dolfing J, Guo Z, Chen R, Wu M, Li Z, Lin X, and Feng Y. 2021. Important
516   ecophysiological roles of non-dominant Actinobacteria in plant residue decomposition,
517   especially in less fertile soils. *Microbiome* 9:1-17.

518 Barathi S, Karthik C, Nadanasabapathi S, and Padikasan IA. 2020. Biodegradation of textile dye
519   Reactive Blue 160 by Bacillus firmus (Bacillaceae: Bacillales) and non-target toxicity
520   screening of their degraded products. *Toxicology reports* 7:16-22.
521 Bello-Akinosho M, Makofane R, Adeleke R, Thantsha M, Pillay M, and Chirima GJ. 2016.
522   Potential of polycyclic aromatic hydrocarbon-degrading bacterial isolates to contribute to
523   soil fertility. *BioMed Research International* 2016.
524 Bolyen E, Rideout JR, Dillon MR, Bokulich NA, Abnet CC, Al-Ghalith GA, Alexander H, Alm
525   EJ, Arumugam M, and Asnicar F. 2019. Reproducible, interactive, scalable and
526   extensible microbiome data science using QIIME 2. *Nature biotechnology* 37:852-857.
527 Busse H-J, Denner EB, Buczolits S, Salkinoja-Salonen M, Bennasar A, and Kämpfer P. 2003.
528   Sphingomonas aurantiaca sp. nov., Sphingomonas aerolata sp. nov. and Sphingomonas
529   faeni sp. nov., air-and dustborne and Antarctic, orange-pigmented, psychrotolerant
530   bacteria, and emended description of the genus Sphingomonas. *International journal of*
531   *systematic and evolutionary microbiology* 53:1253-1260.
532 Chan Y, Van Nostrand JD, Zhou J, Pointing SB, and Farrell RL. 2013. Functional ecology of an
533   Antarctic dry valley. *Proceedings of the National Academy of Sciences* 110:8990-8995.
534 Chen J, Elsgaard L, van Groenigen KJ, Olesen JE, Liang Z, Jiang Y, Lærke PE, Zhang Y, Luo
535   Y, and Hungate BA. 2020a. Soil carbon loss with warming: New evidence from
536   carbon-degrading enzymes. *Global change biology* 26:1944-1952.
537 Chen M, Liu H, Yu S, Wang M, Pan L, Chen N, Wang T, Chi X, and Du B. 2020b. Long-term
538   continuously monocropped peanut significantly changed the abundance and composition
539   of soil bacterial communities. *PeerJ* 8:e9024.
540 Chen W, Teng Y, Li Z, Liu W, Ren W, Luo Y, and Christie P. 2018. Mechanisms by which
541   organic fertilizer and effective microbes mitigate peanut continuous cropping yield
542   constraints in a red soil of south China. *Applied Soil Ecology* 128:23-34.
543 Cherven K. 2013. *Network graph analysis and visualization with Gephi*: Packt Publishing Ltd.
544 Conthe M, Wittorf L, Kuenen JG, Kleerebezem R, van Loosdrecht MC, and Hallin S. 2018. Life
545   on N 2 O: deciphering the ecophysiology of N 2 O respiring bacterial communities in a
546   continuous culture. *The ISME Journal* 12:1142-1153.
547 Devi S, Abdul Rehman SA, Tarique KF, and Gourinath S. 2017. Structural characterization and
548   functional analysis of cystathionine β-synthase: an enzyme involved in the reverse
549   transsulfuration pathway of Bacillus anthracis. *The FEBS journal* 284:3862-3880.
550 Edgar RC. 2018. Updating the 97% identity threshold for 16S ribosomal RNA OTUs.
551   *Bioinformatics* 34:2371-2375.
552 Fierer N, Bradford MA, and Jackson RB. 2007. Toward an ecological classification of soil
553   bacteria. *Ecology* 88:1354-1364.
554 Fox EM, and Howlett BJ. 2008. Secondary metabolism: regulation and role in fungal biology.
555   *Current opinion in microbiology* 11:481-487.
556 Gao Z, Han M, Hu Y, Li Z, Liu C, Wang X, Tian Q, Jiao W, Hu J, and Liu L. 2019. Effects of
557   continuous cropping of sweet potato on the fungal community structure in rhizospheric
558   soil. *Frontiers in microbiology* 10:2269.
559 Gobet A, Quince C, and Ramette A. 2010. Multivariate Cutoff Level Analysis (MultiCoLA) of
560   large community data sets. *Nucleic acids research* 38:e155-e155.
561 Han G, Lan J, Chen Q, Yu C, and Bie S. 2017. Response of soil microbial community to
562   application of biochar in cotton soils with different continuous cropping years. *Scientific*
563   *reports* 7:1-11.

564   Hou F, Du J, Yuan Y, Wu X, and Zhao S. 2021. Analysis of Microbial Communities in Aged
565   Refuse Based on 16S Sequencing. *Sustainability* 13:4111.
566   Huang L-F, Song L-X, Xia X-J, Mao W-H, Shi K, Zhou Y-H, and Yu J-Q. 2013. Plant-soil
567   feedbacks and soil sickness: from mechanisms to application in agriculture. *Journal of*
568   *chemical ecology* 39:232-242.
569   Khurana H, Sharma M, Verma H, Lopes BS, Lal R, and Negi RK. 2020. Genomic insights into
570   the phylogeny of Bacillus strains and elucidation of their secondary metabolic potential.
571   *Genomics* 112:3191-3200.
572   Kumar P, Khare S, and Dubey R. 2012. Diversity of bacilli from disease suppressive soil and
573   their role in plant growth promotion and yield enhancement. *New York Sci J* 5:90-111.
574   Kuzyakov Y. 2010. Priming effects: Interactions between living and dead organic matter. *Soil*
575   *Biology and Biochemistry* 42:1363-1371.
576   Lal R. 2016. Soil health and carbon management. *Food and Energy Security* 5:212-222.
577   Li Y, Chi J, Ao J, Gao X, Liu X, Sun Y, and Zhu W. 2021. Effects of Different Continuous
578   Cropping Years on Bacterial Community and Diversity of Cucumber Rhizosphere Soil in
579   Solar-Greenhouse. *Current Microbiology* 78:2380-2390.
580   Liu Z, Liu J, Yu Z, Yao Q, Li Y, Liang A, Zhang W, Mi G, Jin J, and Liu X. 2020. Long-term
581   continuous cropping of soybean is comparable to crop rotation in mediating microbial
582   abundance, diversity and community composition. *Soil and Tillage Research*
583   197:104503.
584   Loiret F, Ortega E, Kleiner D, Ortega-Rodés P, Rodes R, and Dong Z. 2004. A putative new
585   endophytic nitrogen-fixing bacterium Pantoea sp. from sugarcane. *Journal of applied*
586   *microbiology* 97:504-511.
587   Lourenço KS, Cassman NA, Pijl AS, van Veen JA, Cantarella H, and Kuramae EE. 2018.
588   Nitrosospira sp. govern nitrous oxide emissions in a tropical soil amended with residues
589   of bioenergy crop. *Frontiers in microbiology* 9:674.
590   Magoč T, and Salzberg SL. 2011. FLASH: fast length adjustment of short reads to improve
591   genome assemblies. *Bioinformatics* 27:2957-2963.
592   Meola M, Lazzaro A, and Zeyer J. 2014. Diversity, resistance and resilience of the bacterial
593   communities at two alpine glacier forefields after a reciprocal soil transplantation.
594   *Environmental microbiology* 16:1918-1934.
595   Meyer N, Welp G, Rodionov A, Borchard N, Martius C, and Amelung W. 2018. Nitrogen and
596   phosphorus supply controls soil organic carbon mineralization in tropical topsoil and
597   subsoil. *Soil Biology and Biochemistry* 119:152-161.
598   Murphy CE, and Lemerle D. 2006. Continuous cropping systems and weed selection. *Euphytica*
599   148:61-73.
600   Nassar HN, El-Gendy NS, Mostafa Y, Mahdy H, and El-Temtamy S. 2013. Desulfurization of
601   dibenzothiophene by a novel strain Brevibacillus invocatus C19 isolated from Egyptian
602   coke. *Biosciences Biotechnology Research Asia* 10.
603   Oksanen J, Blanchet FG, Kindt R, Legendre P, Minchin PR, O'hara R, Simpson GL, Solymos P,
604   Stevens MHH, and Wagner H. 2013. Package 'vegan'. *Community ecology package,*
605   *version* 2:1-295.
606   Pang Z, Dong F, Liu Q, Lin W, Hu C, and Yuan Z. 2021. Soil metagenomics reveals effects of
607   continuous sugarcane cropping on the structure and functional pathway of rhizospheric
608   microbial community. *Frontiers in microbiology* 12:369.

609 Pervaiz ZH, Iqbal J, Zhang Q, Chen D, Wei H, and Saleem M. 2020. Continuous cropping alters
610   multiple biotic and abiotic indicators of soil health. *Soil Systems* 4:59.
611 Pii Y, Borruso L, Brusetti L, Crecchio C, Cesco S, and Mimmo T. 2016. The interaction between
612   iron nutrition, plant species and soil type shapes the rhizosphere microbiome. *Plant*
613   *Physiology and Biochemistry* 99:39-48.
614 Pinton R, Varanini Z, and Nannipieri P. 2007. *The rhizosphere: biochemistry and organic*
615   *substances at the soil-plant interface*: CRC press.
616 Quast C, Pruesse E, Yilmaz P, Gerken J, Schweer T, Yarza P, Peplies J, and Glöckner FO. 2012.
617   The SILVA ribosomal RNA gene database project: improved data processing and web-
618   based tools. *Nucleic acids research* 41:D590-D596.
619 Ransom-Jones E, Jones DL, McCarthy AJ, and McDonald JE. 2012. The Fibrobacteres: an
620   important phylum of cellulose-degrading bacteria. *Microbial ecology* 63:267-281.
621 Rinot O, Levy GJ, Steinberger Y, Svoray T, and Eshel G. 2019. Soil health assessment: A
622   critical review of current methodologies and a proposed new approach. *Science of the*
623   *Total Environment* 648:1484-1491.
624 Rosenfeld JS. 2002. Functional redundancy in ecology and conservation. *Oikos* 98:156-162.
625 Rotaru A-E, Shrestha PM, Liu F, Ueki T, Nevin K, Summers ZM, and Lovley DR. 2012.
626   Interspecies electron transfer via hydrogen and formate rather than direct electrical
627   connections in cocultures of Pelobacter carbinolicus and Geobacter sulfurreducens.
628   *Applied and environmental microbiology* 78:7645-7651.
629 Schad P, and Spaargaren O. 2006. *World reference base for soil resources 2006: A framework*
630   *for international classification, correlation and communication*: Food and agriculture
631   organization of the United nations (FAO).
632 Shannon P, Markiel A, Ozier O, Baliga NS, Wang JT, Ramage D, Amin N, Schwikowski B, and
633   Ideker T. 2003. Cytoscape: a software environment for integrated models of biomolecular
634   interaction networks. *Genome research* 13:2498-2504.
635 Shen H, Yan W, Yang X, He X, Wang X, Zhang Y, Wang B, and Xia Q. 2020. Co-occurrence
636   network analyses of rhizosphere soil microbial PLFAs and metabolites over continuous
637   cropping seasons in tobacco. *Plant and Soil* 452:119-135.
638 Sheng Z, Van Nostrand JD, Zhou J, and Liu Y. 2015. The effects of silver nanoparticles on intact
639   wastewater biofilms. *Frontiers in microbiology* 6:680.
640 Singh P, Singh RK, Li H-B, Guo D-J, Sharma A, Lakshmanan P, Malviya MK, Song X-P,
641   Solanki MK, and Verma KK. 2020. Diazotrophic bacteria Pantoea dispersa and
642   Enterobacter asburiae promote sugarcane growth by inducing nitrogen uptake and
643   defense-related gene expression. *Frontiers in microbiology* 11.
644 Sun J, Zou L, Li W, Wang Y, Xia Q, and Peng M. 2018. Soil microbial and chemical properties
645   influenced by continuous cropping of banana. *Scientia Agricola* 75:420-425.
646 Swenson TL, Jenkins S, Bowen BP, and Northen TR. 2015. Untargeted soil metabolomics
647   methods for analysis of extractable organic matter. *Soil Biology and Biochemistry*
648   80:189-198.
649 Talwar C, Nagar S, Kumar R, Scaria J, Lal R, and Negi RK. 2020. Defining the environmental
650   adaptations of genus Devosia: Insights into its expansive short peptide transport system
651   and positively selected genes. *Scientific reports* 10:1-18.
652 van Dam NM, and Bouwmeester HJ. 2016. Metabolomics in the rhizosphere: tapping into
653   belowground chemical communication. *Trends in plant science* 21:256-265.

654 Wang Q, Li Z, Li X, Ping Q, Yuan X, Agathokleous E, and Feng Z. 2021. Interactive effects of
655   ozone exposure and nitrogen addition on the rhizosphere bacterial community of poplar
656   saplings. *Science of the Total Environment* 754:142134.
657 Wang Y, Zhu S, Liu T, Guo B, Li F, and Bai X. 2020. Identification of the rhizospheric microbe
658   and metabolites that led by the continuous cropping of ramie (Boehmeria nivea L. Gaud).
659   *Scientific reports* 10:1-11.
660 Withers E, Hill PW, Chadwick DR, and Jones DL. 2020. Use of untargeted metabolomics for
661   assessing soil quality and microbial function. *Soil Biology and Biochemistry* 143:107758.
662 Wu Y-F, Chai C-W, Li Y-N, Chen J, Yuan Y, Hu G, Rosen BP, and Zhang J. 2021. Anaerobic
663   As (III) oxidation coupled with nitrate reduction and attenuation of dissolved Arsenic by
664   Noviherbaspirillum Species. *ACS Earth and Space Chemistry* 5:2115-2123.
665 Wunder LC, Aromokeye DA, Yin X, Richter-Heitmann T, Willis-Poratti G, Schnakenberg A,
666   Otersen C, Dohrmann I, Römer M, and Bohrmann G. 2021. Iron and sulfate reduction
667   structure microbial communities in (sub-) Antarctic sediments. *The ISME Journal*:1-18.
668 Xi H, Shen J, Qu Z, Yang D, Liu S, Nie X, and Zhu L. 2019. Effects of long-term cotton
669   continuous cropping on soil microbiome. *Scientific reports* 9:1-11.
670 Yan L, Zhang W, Duan W, Zhang Y, Zheng W, and Lai X. 2021. Temporal Bacterial
671   Community Diversity in the Nicotiana tabacum Rhizosphere Over Years of Continuous
672   Monocropping. *Frontiers in microbiology* 12:1276.
673 Yang C, Liu N, and Zhang Y. 2019. Soil aggregates regulate the impact of soil bacterial and
674   fungal communities on soil respiration. *Geoderma* 337:444-452.
675 Yao Y, Yao X, An L, Bai Y, Xie D, and Wu K. 2020. Rhizosphere Bacterial Community
676   Response to Continuous Cropping of Tibetan Barley. *Frontiers in microbiology*
677   11:551444-551444.
678 Yu L, Tang Y, Wang Z, Gou Y, and Wang J. 2019. Nitrogen-cycling genes and rhizosphere
679   microbial community with reduced nitrogen application in maize/soybean strip
680   intercropping. *Nutrient Cycling in Agroecosystems* 113:35-49.
681 Zeng Q, and An S. 2021. Identifying the Biogeographic Patterns of Rare and Abundant Bacterial
682   Communities Using Different Primer Sets on the Loess Plateau. *Microorganisms* 9:139.
683 Zhang Y, Li P, Liu X, Xiao L, Shi P, and Zhao B. 2019. Effects of farmland conversion on the
684   stoichiometry of carbon, nitrogen, and phosphorus in soil aggregates on the Loess Plateau
685   of China. *Geoderma* 351:188-196.
686 Zhao J, Zhang D, Yang Y, Pan Y, Zhao D, Zhu J, Zhang L, and Yang Z. 2020. Dissecting the
687   effect of continuous cropping of potato on soil bacterial communities as revealed by
688   high-throughput sequencing. *PloS one* 15:e0233356.
689 Zhao Y, Fu W, Hu C, Chen G, Xiao Z, Chen Y, Wang Z, and Cheng H. 2021. Variation of
690   rhizosphere microbial community in continuous mono-maize seed production. *Scientific*
691   *reports* 11:1-13.
692 Zheng B, Zhu Y, Sardans J, Peñuelas J, and Su J. 2018. QMEC: a tool for high-throughput
693   quantitative assessment of microbial functional potential in C, N, P, and S
694   biogeochemical cycling. *Science China Life Sciences* 61:1451-1462.
695 Zhou Z, Tran PQ, Kieft K, and Anantharaman K. 2020. Genome diversification in globally
696   distributed novel marine Proteobacteria is linked to environmental adaptation. *The ISME*
697   *Journal* 14:2060-2077.
698

Figure 1

Total 20 taxa showed significant feedback continuously strengthening or weakening to the long-term monocropping of Tibetan barley. (A) 10 taxa were increased, while (B) 10 taxa were decreased.

The correlation between the relative abundance of each taxon and enhanced cropping yeas was further validated by ANOVA. *P* < 0.05 was considered significant.
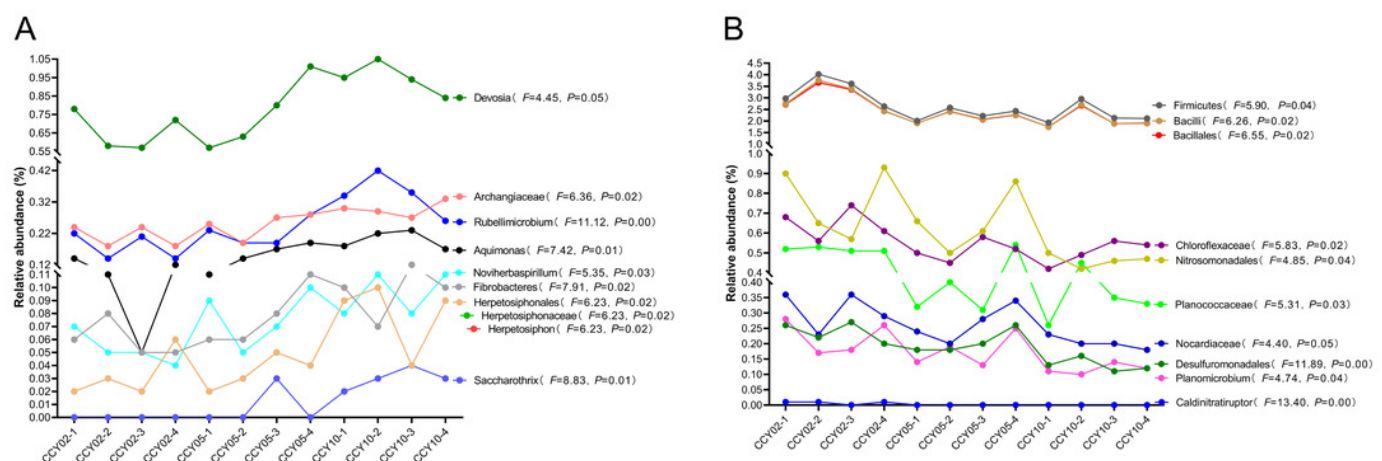
Figure 2

The relative contribution of main genera to the dissimilarity between communities of (A) CCY02 and CCY05, (B) CCY02 and CCY10, and (C) CCY05 and CCY10 by SIMPER analysis.

The main genera was listed when cumulative dissimilarity over 50% in each group.
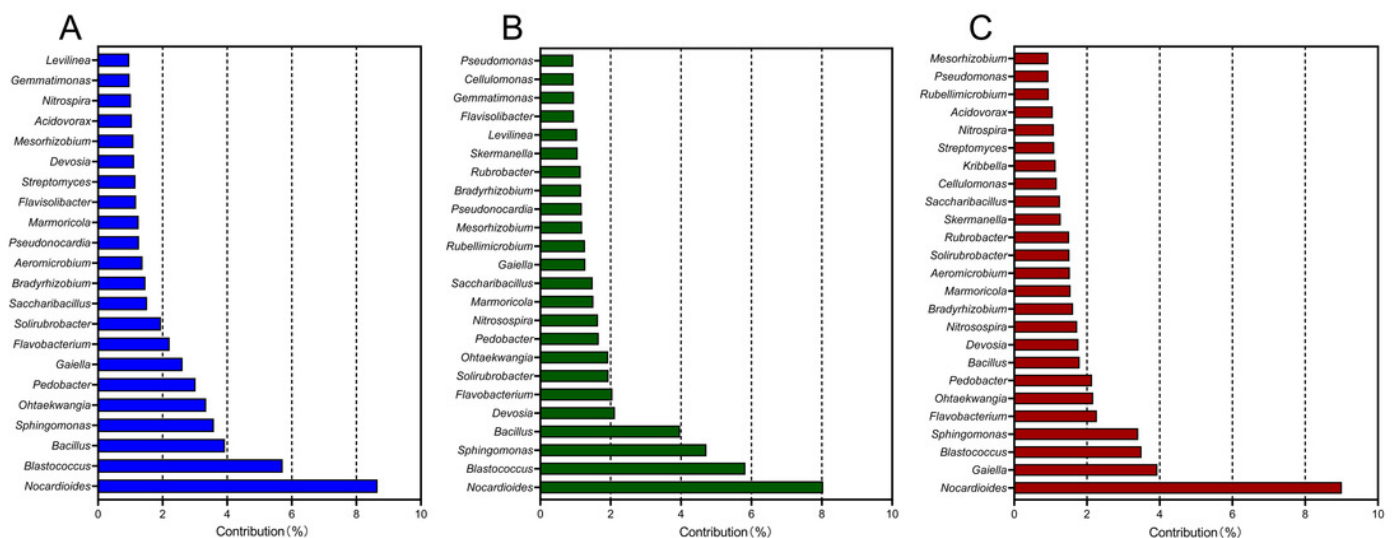
Figure 3

Richness, abundance, and identity of taxa are shared across all rhizosphere soil samples. (A) Richness and sequence coverage of shared taxa in all the samples. (B) Heatmap of the top 20 shared genera among samples.

Relative abundances were log-transformed and colored from blue to red to indicate high-to-low relative abundances. Shared genera were identified as dominant (>1% relative abundance) or rare (<1% relative abundance) in each group. The name of each genus is colored by phylum class.
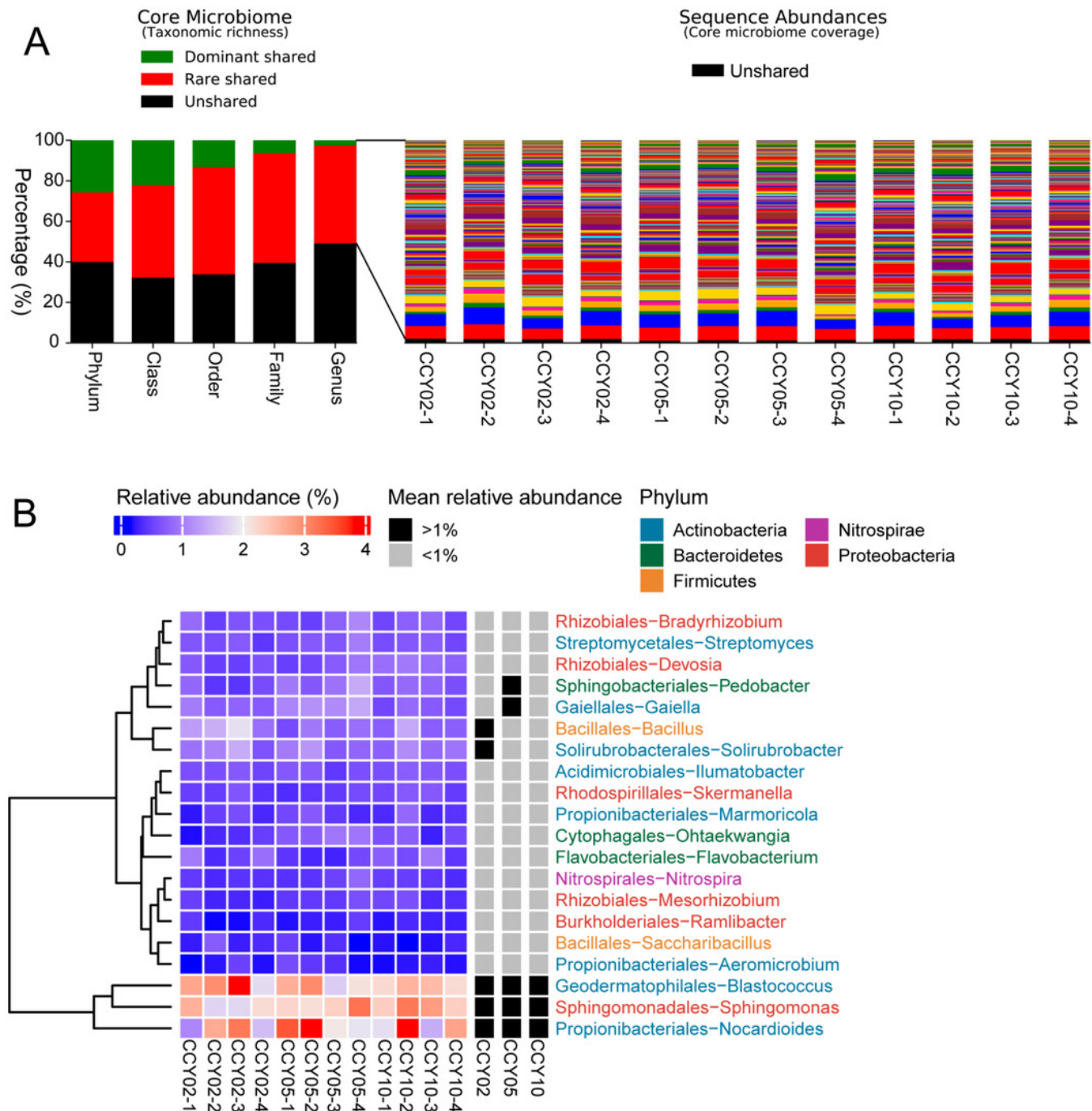
Figure 4

Relationships between bacterial community structure and functional gene profiles from QMEC analysis during (A) long-term and (B) short-term of continuous monocropping years, respectively.

The correlation was determined by Procrustes test and considered significanlt when $P < 0.05$.
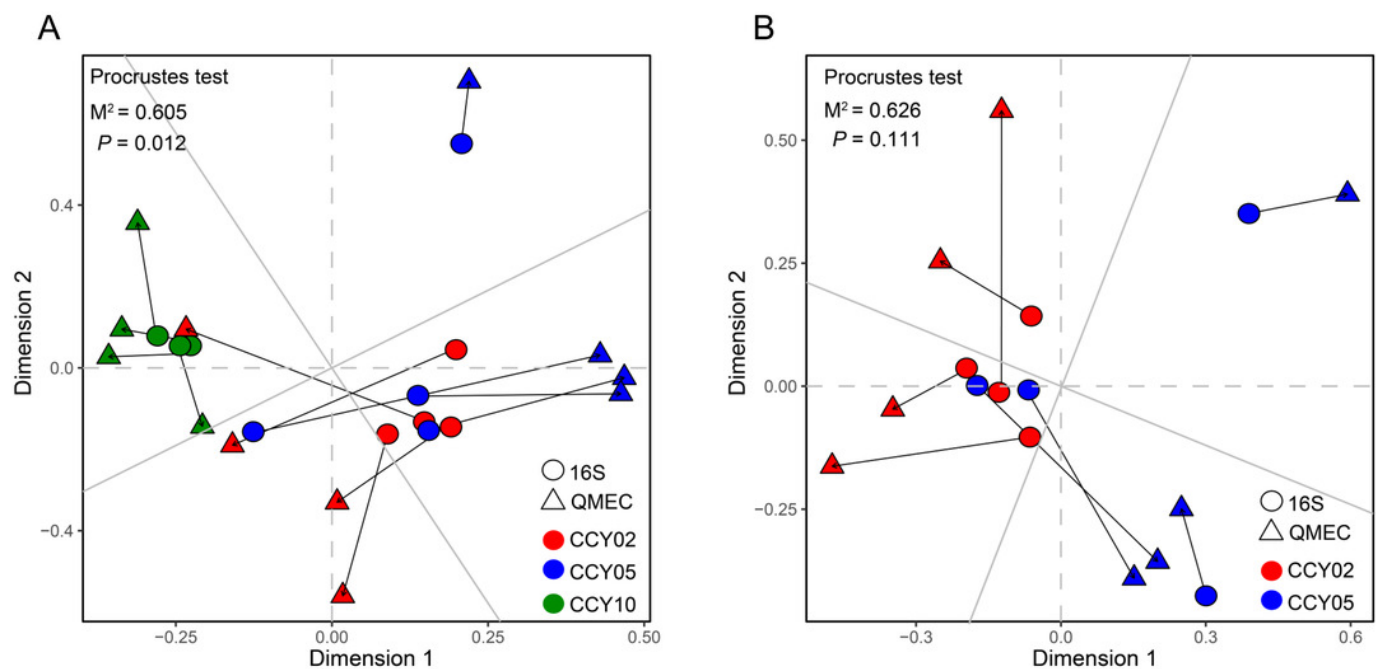
Figure 5

The Co-occurrence network between the functional genes and all the bacterial genera appeared in all rhizosphere soil samples.

A connection indicates a strong ($|r|$ of > 0.6) and significant (P of < 0.05) Spearman's correlation, while only a connection between genera and functional gene was kept. Red lines indicate negative correlations, while green lines indicate positive correlations. The network is colored by module, which clusters the tightly connected nodes. The size of each node is proportional to the number of connections: The thickness of each edge is proportional to the value of the Spearman correlation. The same node colors represent nodes belonging to the same modules. The font color blue represents the functional gene, while the font-weight represents the genera that clustered tightly within Module I with node degrees larger than 10.
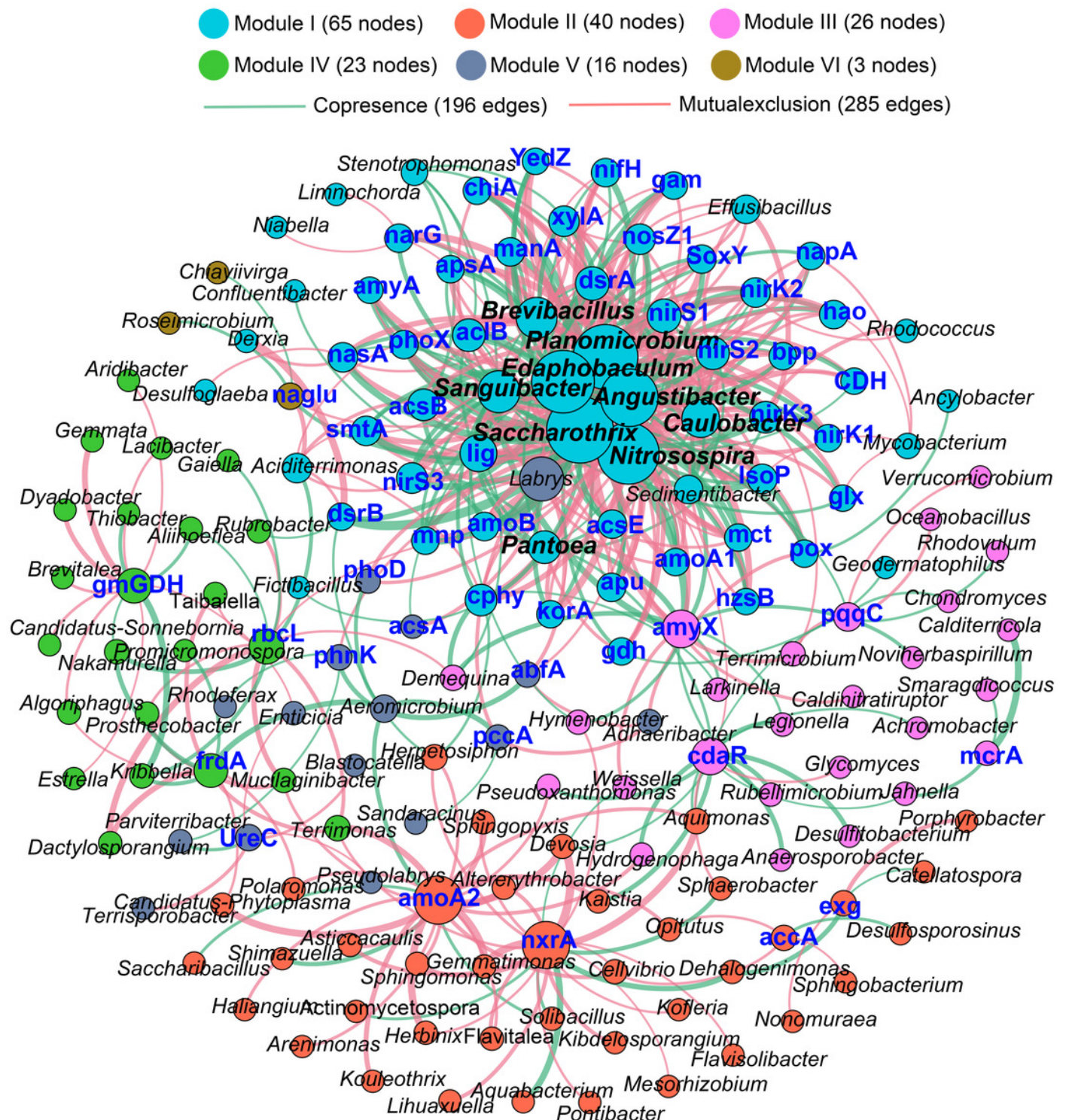
Figure 6

Correlations between the main overlapped genera (detected by SIMPER analysis) with the functional genes in rhizosphere soils.

Heatmap values ranged from +0.5 to -0.5. Values above/below zero represent positive/negative correlations. *$P < 0.05$ was considered significant, while **$P < 0.01$ was considered extremely significant.
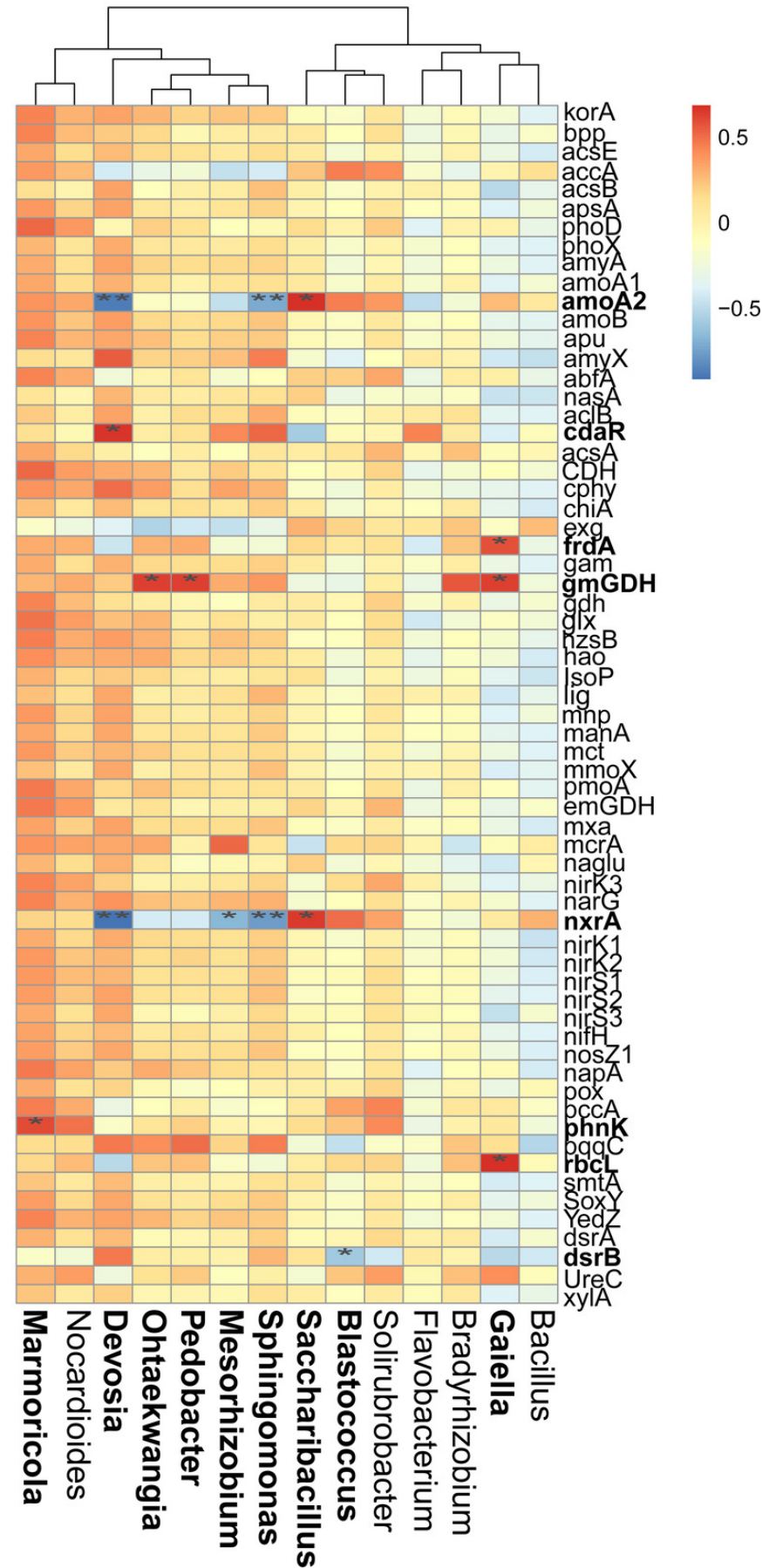
Figure 7

Relationships between bacterial community structure and Functional gene profiles from non-targeted metabolomic analysis during (A) long-term and (B) short-term of continuous monocropping years, respectively.

The correlation was determined by Procrustes test and considered significanlt when *P* < 0.05.

Figure 8

The network between the differential expressed metabolites and differentially abundant genera among different cropping years.

A connection indicates a very strong (|*r*| of > 0.9) and significant (*P* of < 0.01) Spearman's correlation, while only a connection between genera and functional gene was kept. Red lines indicate negative correlations, while green lines indicate positive correlations. The size of each node is proportional to the number of connections: The thickness of each edge is proportional to the value of the Spearman correlation.
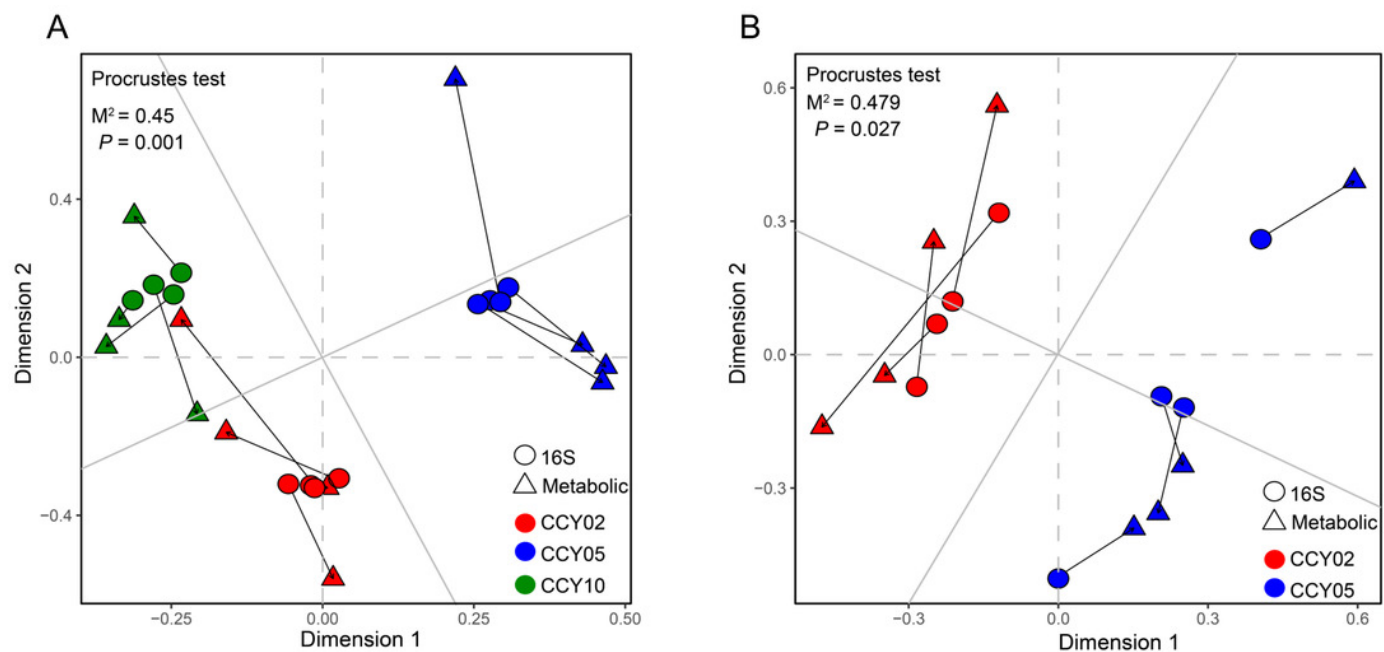
Significant differences of the four alpha indexes among groups.

Values represent the mean ± standard deviation (n = 4). Different lowercase letters within the same column indicate significant differences among different continuous cropping years (Kruskal-Wallis, P < 0.05).

1   **Table 1.** Significant differences of the four alpha indexes among groups.

	Chao1	ACE	PD	Shannon
CCY02	4746.71 ± 155.81a	4825.48 ± 137.84a	179.89 ± 7.65a	9.69 ± 0.16ab
CCY05	4344.43 ± 195.09b	4387.67 ± 188.26b	162.66 ± 4.50b	9.51 ± 0.09b
CCY10	4769.57 ± 164.57a	4886.41 ± 137.82a	178.89 ± 3.22a	9.72 ± 0.06a

2   Values represent the mean ± standard deviation (n = 4). Different lowercase letters within the

3   same column indicate significant differences among different continuous cropping years

4   (Kruskal-Wallis, $P < 0.05$).